

# Furazan bis-ureas: a heterocyclic scaffold for anion binding and transport

Received 00th January 20xx,  
Accepted 00th January 20xx

William G. Ryder,<sup>a,b</sup> Emilie G. Wu,<sup>a</sup> Lijun Chen,<sup>c</sup> Mohamed Fares,<sup>a,d</sup> Daniel A. McNaughton,<sup>a,b</sup> Karen Tran,<sup>a</sup> Chengzhong Yu,<sup>c</sup> and Philip A. Gale<sup>\*a,b</sup>

DOI: 10.1039/x0xx00000x

The incorporation of hydrogen bonding motifs surrounding a central cyclic scaffold has proven to be an effective method in the design of synthetic anion transporters. Herein, we report a novel and synthetically accessible architecture centred around an oxadiazole ring. The series was found to effectively mediate the perturbation of liposomal pH gradients at micromolar concentrations *via* a H<sup>+</sup>/Cl<sup>−</sup> transport mechanism and a wide range of cytotoxicities were exhibited against cancerous and normal cell lines.

## Introduction

Supramolecular scaffolds that facilitate anion transmembrane transport have demonstrated their therapeutical application as potential anticancer agents, due to their ability to strategically perturb cellular ionic and pH levels.<sup>1–3</sup>

Over the last two decades, anion receptors have developed to encompass a wide variety of architectures to create the ideal environment for host-guest interactions.<sup>4–12</sup> Anionophoric scaffolds using simple cyclic hydrocarbon or aromatic frameworks have become popular due to their synthetic availability and integral lipophilicity.<sup>13–20</sup> However, increasing the complexity of scaffold design can often be accompanied by long and arduous synthetic pathways.<sup>21</sup> As the field of anion recognition and transmembrane transport progresses towards potential therapeutic applications, there is a growing desire to create effective anionophoric scaffolds that are synthetically accessible.<sup>22</sup>

1,2-Hydrogen bonding motifs centred around cyclic structures have proven to be highly potent anion carriers, but the anion binding and transport ability of these derivatives based around a five-membered ring is relatively unknown.<sup>23–25</sup> The croconamide series provided the first example of an anion receptor employing an *ortho*-hydrogen bonding arrangement around a five-membered scaffold.<sup>26</sup> However, Jolliffe and co-workers highlighted that the potential application of these systems was hindered by the receptor's facile deprotonation, even in the absence of basic species.<sup>27</sup>

To investigate this gap in the architectural chemical space, we chose to implement a 1,2,5-oxadiazole (furazan) ring as a

central scaffold for a series of urea-based transporters. Furazans are a class of highly polarised aromatic heterocycles that have been exploited to act as planar, aromatic linkers which can position pharmacologically active substituents into appropriate orientations.<sup>28–30</sup> Their highly inductive nature is comparable to that of a trifluoromethyl group, which has found extensive use in both anion receptor chemistry and transmembrane transport due to its effect on hydrogen bond strength.<sup>31,32</sup> We anticipated that the geometry of the five-membered ring scaffold, in addition to furazan's unique physical and electronic properties, would offer new insight into the influence of these properties on transmembrane transport.

Herein, we describe the synthesis of nine furazan-based anionophores (**1–9**), each functionalised with a variety of electron-withdrawing substituents to compare the effects of both lipophilicity and hydrogen bond donor strength on transport activity. Single crystal X-ray diffraction highlighted a network of internal hydrogen bonds between the central scaffold and the urea motifs. The moderate binding affinity of the series to Cl<sup>−</sup> compared to similar dual-urea scaffolds was attributed to these competitive interactions. Each receptor demonstrated the ability to mediate H<sup>+</sup>/Cl<sup>−</sup> transport in both potentiometric- and fluorescence-based liposomal assays. Moreover, treatment of the receptors to cancerous and normal cell lines was found to elicit a range of cytotoxicity.

## Results and discussion

### Synthesis

The furazan series (**1–9**) was afforded through a one- or two-step synthetic pathway, typically initiated with commercially available 3,4-diaminofurazan (Scheme 1). Compounds **1–6** were synthesised by the addition of the respective isocyanates to 3,4-diaminofurazan in CH<sub>3</sub>CN. The yields of the urea formation varied depended on the degree of fluorination to the peripheral aryl rings, whereby the highly fluorinated moieties typically returned the lowest yields. This was attributed to the increased acidity of the urea motifs, which complicated their purification via chromatographic techniques.

<sup>a</sup> School of Chemistry, The University of Sydney, Sydney, NSW, 2006, Australia.

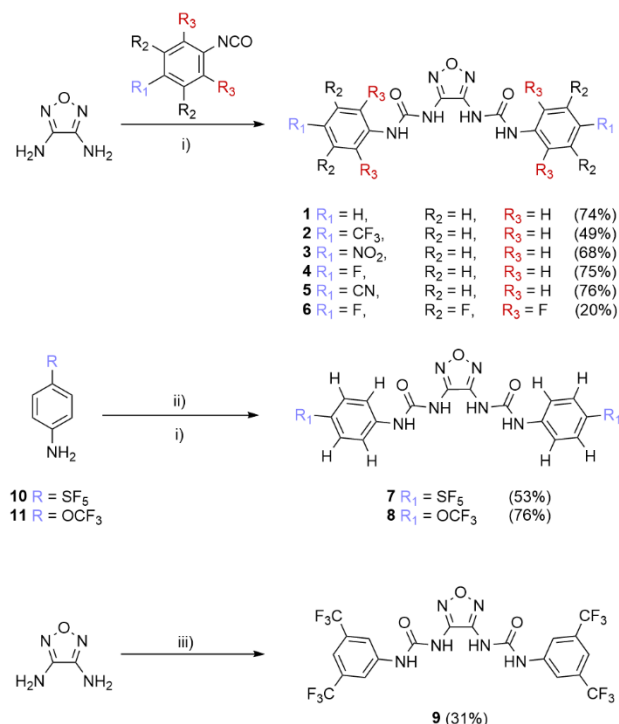
<sup>b</sup> School of Mathematical and Physical Sciences, Faculty of Science, University of Technology Sydney, Ultimo, NSW 2007, Australia.

<sup>c</sup> Australian Institute for Bioengineering and Nanotechnology, The University of Queensland, Brisbane, QLD, 4072 Australia

<sup>d</sup> School of Pharmacy, The University of Sydney, Sydney, NSW 2006, Australia

† Footnotes relating to the title and/or authors should appear here.

Electronic Supplementary Information (ESI) available: Synthesis and characterisation details, anion binding and transport studies and X-ray crystallography. CCDC 2279691 and CCDC 2279693 For ESI and crystallographic data in CIF or other electronic format. See DOI: 10.1039/x0xx00000x



**Scheme 1** Synthesis of furazan-centred bis-ureas (1–9): i) CH<sub>3</sub>CN, 80 °C; ii) triphosgene, toluene, triethylamine, 70 °C; iii) DMSO, 50 °C.

Compounds **7** and **8** were synthesised from a procedure reported by Gale and co-workers.<sup>33</sup> Triphosgene in dry toluene was treated with the respective aniline (**10** or **11**), and the in-situ generated isocyanate was subsequently added in one portion to 3,4-diaminofurazan in CH<sub>3</sub>CN affording both **7** and **8** in a moderate and good yield, respectively. Due to the difficulty associated with its isolation, an alternate approach was used for the synthesis of **9**. It was found that DMSO at a lower temperature was the most reliable method to afford **9**, which was obtained in a low yield (31%). Detailed synthetic procedures and full characterisation can be found within the ESI.

### X-ray crystallography

Crystals of compound **1** suitable for X-ray diffraction were obtained by slow evaporation of a saturated solution of the receptor in either CH<sub>3</sub>CN or DMSO. Receptor **1** was crystallised as a DMSO solvate (CCDC 2279691, Figure 1a) which contained a network of internal hydrogen bonding interactions. Firstly, the DMSO was shown to be bound to the outwardly facing urea nitrogen donors (N29 and N31) via the O12 sulfoxide acceptor (N–O distances 2.727(3)–2.809(3) Å, N–H···O angles 155.0(2)°–159.7(2)°). The solvent was not bound in the proposed central cavity, possibly due to an additional hydrogen bond of the free urea blocking the binding site. The formation of a pseudocyclic six-membered ring was observed between the outermost urea nitrogen donor, N27, and the furazan nitrogen acceptor N33 (N–N distance 2.731(3) Å, N–H···N angle 139.3(2)°). Within the same urea, the innermost nitrogen, N24, was positioned into the originally proposed cavity, whereby another hydrogen bond is formed between the urea carbonyl acceptor O22 forming a

pseudocyclic seven-membered ring (N–O distance 2.726(2) Å, N–H···O angle 148.7(2)°).

Crystallisation in a less competitive solvent elicited a new conformer of receptor **1**. In CH<sub>3</sub>CN, compound **1** was crystallised as the free receptor (CCDC 2279693, Figure 1b) and again was shown to possess a series of internal hydrogen bonds from both of the outermost urea nitrogen donors, N5 and N24, and the nitrogen acceptors of the furazan scaffold, N7 and N26, (N–N distances 2.705(3) Å, N–H···N angles 138.6(2)°). The formation of the pseudocyclic six membered rings caused the receptor to adopt an *anti-anti* conformation. While the conformation is not preorganised for anion binding, we have previously shown through DFT calculations that intramolecular hydrogen bonds can weaken the NH proton acidity of the *anti-anti* orientation.<sup>34</sup> Hence, the conformers are less able to bind to anions, but can more efficiently partition into the lipid bilayer, resulting in an increase in transmembrane transport ability. Additionally, the intramolecular bond between the NH protons and the furazan ring alters the solvent accessibility of the receptor. The decreased interaction with the solvent may shield the highly polar scaffold in solution, enhancing the lipophilicity of the scaffold. This conformational change may help strike the balance between solubility in both the aqueous solution and the lipid bilayer.

### Anion binding studies

Proton NMR titrations for the series of furazan bis-ureas (**1–9**) were performed with Cl<sup>−</sup> to obtain their respective association constants (K<sub>a</sub>). Significant downfield shifts in the resonances attributed to the urea NH protons was observed for all

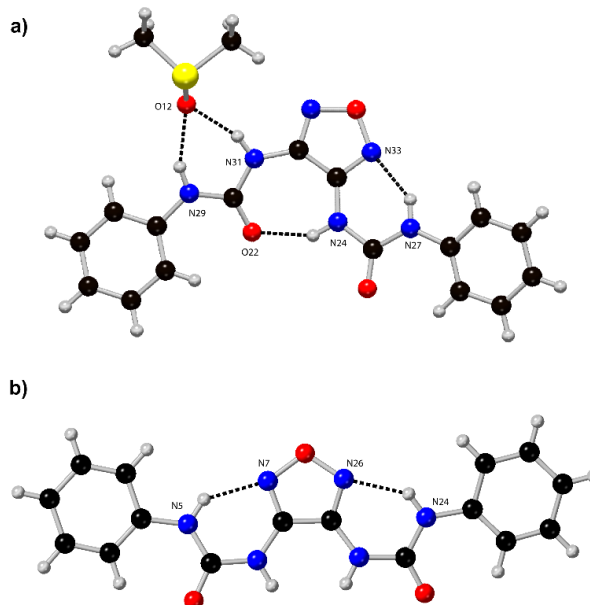


**Figure 1** a) Crystal structure of **1** as a DMSO solvate, highlighting the formation of six- and seven-membered pseudocyclic rings directed by internal hydrogen bonds (dashed lines) of the ureas and the furazan scaffold.; b) X-ray crystal structure of **1** in CH<sub>3</sub>CN, forming two symmetrical six-membered pseudocyclic rings dictated by internal hydrogen bonding (dashed lines).

receptors upon the addition of tetrabutylammonium chloride (TBACl) (Figure S30–S54†). Proton NMR titrations for the series of furazan bis-ureas (**1–9**) were performed with chloride to obtain their respective association constants ( $K_a$ ). Significant downfield shifts in the resonances attributed to the urea NH protons was observed for all receptors upon the addition of tetrabutylammonium chloride (TBACl). It should be noted that the  $K_a$  for receptor **6** could not be reliably determined due to significant broadening of the NH resonances in the presence of increased concentrations of the anion (Figure S45†).  $K_a$  values for the remaining receptors were obtained by global fitting of the two urea NH resonances to various receptor:anion binding models using the Bindfit applet.<sup>35,36</sup> Fitting to a 1:1 receptor:guest model resulted in a poor fit for the majority of the receptors and significantly better fitting was observed when a 1:2 receptor:guest model was used. The  $F_{covfit}$  was calculated for each of the receptors and the covariance of fit of the 1:2 binding model was found to be at least eight times greater for all receptors, with the exception of receptor **1** which showed no preference for either model. The association constants for all binding models and  $F_{covfit}$  are shown in Table 1.

The assessment of the  $K_{11}$  values showed that all the receptors exhibited weak to moderate binding towards chloride. Due to the observed 1:2 binding mode, the anion binding affinity of the library was assessed using the calculated product of the  $K_{11}$  and  $K_{12}$  values (overall stability constant,  $\beta$ ). Hammett constants ( $\sigma_p$ ) are a good descriptor in quantifying electron-withdrawing effects, and in general, the receptors with the strongest electron-withdrawing substituents on the peripheral phenyl ring demonstrated the highest binding.<sup>37</sup> The parent phenyl receptor **1**, with no electron withdrawing substituents, displayed the weakest binding. Enhancements in the binding ability were observed through the addition of fluorinated motifs shown by receptors **4** and **8**. Higher stability constants were determined for receptor **7** over compounds **2**, **5**, and **3**. The strongest binding was shown by receptor **9**, which was appended with highly electron-withdrawing bis-trifluoromethyl groups, that can greatly enhance the hydrogen bond strength,

enabling the strongest interactions with  $Cl^-$ . The rotational flexibility of the ureido motif around the furazan scaffold allows for different conformations. We initially theorised that the free receptor was unlikely to exist in the *syn–syn* conformation due to the electrostatic repulsion between the lone pairs of the carbonyl groups and the nitrogen atoms on the furazan ring. However, 2D NOESY  $^1H$  NMR experiments conducted with receptors **1–9** revealed NOE cross-peaks between the resonances attributed to both NH urea protons (Figure S73–S90†), indicating a dominant *syn–syn* conformation of the free receptors in solution (Figure 2). In the presence of an anion, it was anticipated that the receptors would continue to adopt the observed *syn–syn* conformation where all four urea NH protons form a convergent hydrogen bonding array towards the anion, maximising anion–receptor interactions. However, the crystal structures of receptor **1** highlighted an *anti–anti* conformation of both the free and DMSO-solvated receptor. Both solid-state structures demonstrated an internal hydrogen bonding network which fixed the ureas in a conformation detrimental to intermolecular binding with an anionic guest. Two NH urea protons can be found below the furazan scaffold in the *anti–anti* conformation (highlighted in red in Figure 2); however, this unique orientation and high convergence of the NH protons may not provide a suitable geometric match to spherical anionic guests when compared to a single urea motif.<sup>39</sup> Further evidence of the binding conformation was evaluated using the  $^1H$  NMR spectra of the titrations with  $Cl^-$ . Both sets of urea NH resonance signals were found to shift downfield, indicating that each NH proton on the same urea is involved in the same binding event. If the *anti–anti* conformation displayed by the free receptor was the favoured binding conformation, perturbation of one NH resonance per urea (highlighted in red in Figure 2) would be observed on the  $^1H$  NMR spectra. Further assessment of the  $^1H$  NMR spectra showed that a single binding species was maintained throughout the titration, and no complex species of a higher order were observed up to the addition of 150 equiv. of TBACl and led to the proposed symmetrical 1:2 binding mode of  $[9\cdot 2Cl]^{2-}$  (Figure 2).

The interaction parameter ( $\alpha$ ) values were less than one for all receptors, indicating that the 1:1 complex is heavily favoured over the 1:2 complex.<sup>36</sup> This can be explained through the two conformational changes required for the second complexation of  $Cl^-$ . To free the second binding site, a ‘flip’ of the free binding motif ( $[9\cdot Cl]^-$ , shown in blue Figure 2) is required to present both NH protons into an outward-facing orientation. Secondly, both ureas must rotate away from each other to minimise the lone pair repulsion between the two carbonyl groups and steric encumbrance between the bis-trifluoromethyl moieties ( $[9\cdot 2Cl]^{2-}$ , Figure 2). Furthermore, the receptor is not large enough or geometrically tailored to satisfy the additional anionic charge from the second binding event. Taken together with the increase in free energy needed to generate the optimal binding conformation, this offers a rationalisation of the moderate  $Cl^-$  binding demonstrated by the furazan bis-ureas.

**Table 1** Apparent association constants for receptors **1–9** with  $Cl^-$  (as its TBA salt) in DMSO- $d_6$ /0.5%  $H_2O$

Compound	$K_{11}^a$	$K_{12}^a$	$\beta^b$	$\sigma_p$	$\alpha^c$	$F_{covfit}^f$
<b>1</b>	42	2	89	0.00 <sup>c</sup>	0.21	1
<b>2</b>	219	4	876	0.54 <sup>c</sup>	0.08	58
<b>3</b>	196	5	1062	0.78 <sup>c</sup>	0.11	10
<b>4</b>	85	3	270	0.06 <sup>c</sup>	0.15	9
<b>5</b>	206	5	1033	0.66 <sup>c</sup>	0.10	9
<b>7</b>	211	5	1142	0.61 <sup>c</sup>	0.10	24
<b>8</b>	156	3	529	0.35 <sup>c</sup>	0.09	19
<b>9</b>	220	7	1581	0.85 <sup>d</sup>	0.13	12

<sup>a</sup> ( $M^{-1}$ ) All errors <8% and calculated using a 1:2 binding model from the online BindFit applet. <sup>b</sup> Overall stability constant ( $\beta$ ) is given by  $\beta (M^{-2}) = K_{11}K_{12}$ . <sup>c</sup> Value taken from reference [20].<sup>37</sup> <sup>d</sup> Values taken from reference [21], calculated from the pKa of 3,5-bis- $CF_3$  benzoic acid.<sup>38</sup> <sup>e</sup> The interaction parameter ( $\alpha$ ) calculated by multiplying  $K_{21}$  by 4 and dividing by  $K_{11}$ . A value of  $\alpha < 1$  is indicative of negative cooperativity. <sup>f</sup> Factor of covariance of fit ( $F_{covfit}$ ) calculated by dividing covfit 1:2 with covfit 1:1; a value greater than 5 indicates a favoured 1:2 binding model.

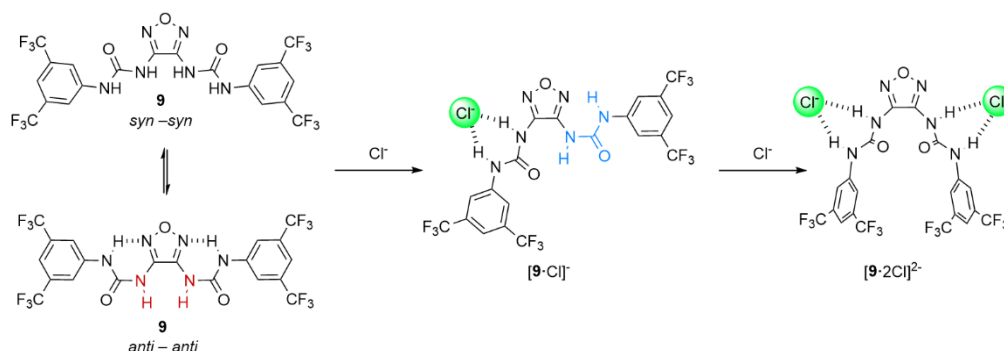


**Figure 2** General schematic of the proposed binding modes of the furazan bis-ureas, using receptor **9** as an example. Dashed lines represent hydrogen bonds.

## Anion transport studies

### Cationophore coupled transport assay

Confirmation of the anion binding capabilities using the five-membered scaffold prompted an investigation into the anionophoric ability of the library. The transport mechanism facilitated by the furazan bis-ureas was assessed using the cationophore coupled assay (Figure 3). The assay utilises natural ionophores valinomycin (a strict  $\text{K}^+$  uniporter) and monensin (a  $\text{K}^+/\text{H}^+$  antiporter). 1-Palmitoyl-2-oleoyl-*sn*-glycero-3-phosphocholine (POPC) large unilamellar vesicles (LUVs, 200 nm) were loaded with KCl (300 mM) and buffered to pH 7.2 using phosphate salts. The vesicles were subsequently suspended in potassium gluconate (KGlu, 300 mM), similarly buffered to pH 7.2 using phosphate salts. Gluconate is a large, highly polar, and hydrophilic anion that cannot be transported across the membrane by an anionophore. Therefore, the addition of the anionophore alone will not initiate  $\text{Cl}^-$  transport as there is no counterflow to alleviate the build-up of negative charge. If the anionophore functions as an electrogenic transporter ( $\text{Cl}^-$  uniport), the addition of valinomycin will increase the rate of transport as the back transport of  $\text{K}^+$  by the cationophore can dissipate the electrochemical gradient generated by  $\text{Cl}^-$  efflux (Figure 3a). Conversely, the addition of monensin will increase the transport rate for an electroneutral transporter ( $\text{H}^+/\text{Cl}^-$  symport or equivalent  $\text{Cl}^-/\text{OH}^-$  antiport) as the  $\text{K}^+/\text{H}^+$  antiport allows the back transport of protons, dissipating the built-up pH gradient (Figure 3b).

The cationophores were added as a 0.1 mol% (with respect to lipid concentration) loading at  $t = -30$  s which allowed for their homogenous distribution. The transporters were added as a DMSO solution (10  $\mu\text{L}$ ) at  $t = 0$  s to initiate efflux, and the increase in  $\text{Cl}^-$  concentrations in the external solution was measured using a  $\text{Cl}^-$  ion selective electrode (ISE). The vesicles were treated with Triton X-100 at  $t = 300$  s to lyse all contents into the external solution and calibrate the 100%  $\text{Cl}^-$  efflux value.

Enhanced  $\text{Cl}^-$  efflux was observed in the presence of monensin for all receptors. In general, most of the receptors exhibited no coupling to valinomycin. For highly fluorinated compounds **6** and **7**, a discernible increase in  $\text{Cl}^-$  efflux was observed in the presence of valinomycin, indicating the facilitation of electrogenic and electroneutral  $\text{Cl}^-$  transport (Figure 4).

However, the observed magnitude of electrogenic transport was far smaller than the corresponding electroneutral transport, revealing a preference for  $\text{H}^+/\text{Cl}^-$  cotransport. An electroneutral transport mechanism was observed for the remaining receptors, where little to no coupling to valinomycin was observed (Figure 4).

Lipophilicity has proven to be a crucial component in the design of synthetic anion transporters.<sup>32,40-42</sup> It is widely recognised that highly fluorinated receptors possess a greater lipophilicity than their non-fluorinated counterparts.

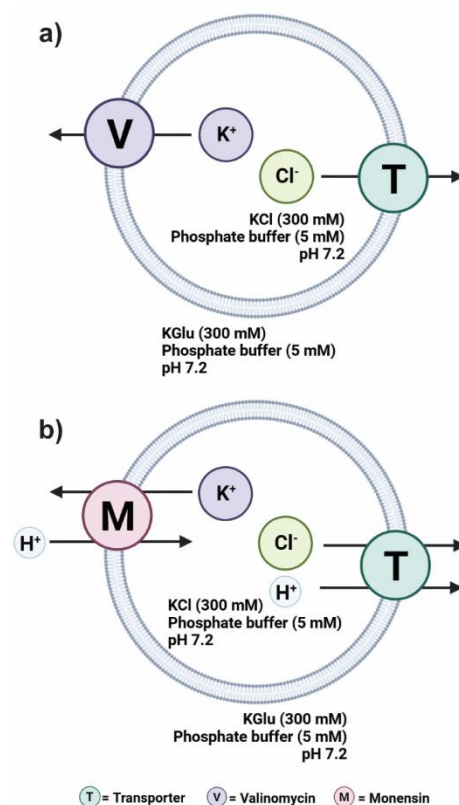


**Figure 3** Schematic of the cationophore coupled assay, monitored by chloride-ISE. POPC vesicles were loaded with phosphate buffered KCl (300 mM) and then suspended in phosphate buffered KGlu (300 mM) adjusted to pH 7.2. Diagrams show (a) overall KCl efflux induced by valinomycin's (V) electrogenic  $\text{K}^+$  transport coupled to the anionophore's electrogenic  $\text{Cl}^-$  transport resulting in an overall electroneutral KCl efflux and (b) overall KCl efflux induced by monensin's (M) electroneutral  $\text{K}^+/\text{H}^+$  exchange and the transporter's  $\text{H}^+/\text{Cl}^-$  cotransport (or equivalent  $\text{Cl}^-/\text{OH}^-$  exchange).

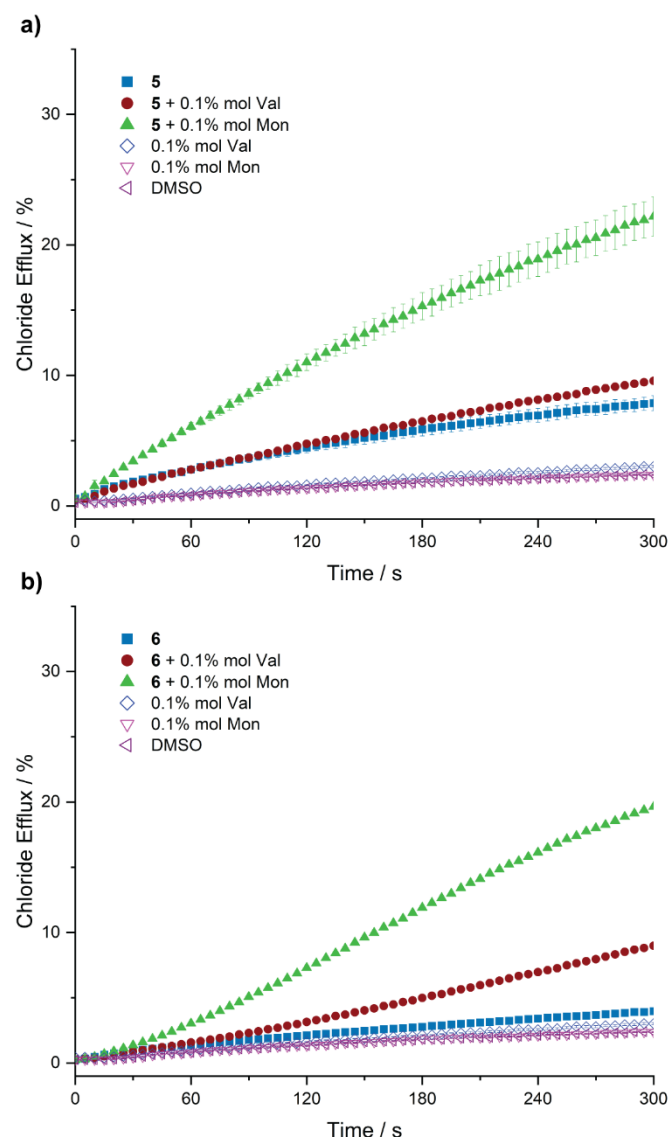


**Figure 5** The  $\text{Cl}^-$  efflux facilitated by a) **5** (10 mol%) and b) **6** (10 mol%) in POPC vesicles loaded with KCl (300 mM) and suspended in an isotonic external solution containing KGLu (300 mM) in the presence of 0.1 mol% monensin (green), 0.1 mol% valinomycin (red) and alone (blue).

Calculated octanol/water partition coefficients (ClogP) values are used to measure the degree of lipophilicity, receptors with a lower ClogP indicate a higher lipophilicity. The ClogP values were calculated for receptors **1–9** using the CADD software, Flare, developed by Cresset Group (Table 2). The peripheral phenyl rings of **6** and **7** possessed the highest degrees of fluorination and were found to be the most lipophilic in the series through their respective calculated ClogP values.

Anionophores that facilitate electrogenic transport must be able to passively diffuse back across the membrane as a neutral receptor after the release of  $\text{Cl}^-$ . This key mechanistic step allows for continual membrane depolarisation as the transporter is regenerated at the top of the  $\text{Cl}^-$  concentration gradient. The increased lipophilicity was theorised to enhance the facile translocation of the uncomplexed forms of **6** and **7** across the lipid membrane and, consequently, improve their rates of electrogenic transport.

### Fluorescence-based $\text{H}^+/\text{Cl}^-$ transport assay

The  $\text{H}^+/\text{Cl}^-$  cotransport ability of receptors **1–9** was further evaluated through the 8-hydroxypyrene-1,3,6-trisulfonate (HPTS) fluorescence-based assay (Figure 5).<sup>43</sup> POPC LUVs (200 nm) were loaded with the pH-responsive fluorophore (HPTS) (1 mM) and *N*-methyl-D-glucamine (NMDG) chloride (100 mM), buffered with HEPES (10 mM) to pH 7.0 with HCl. The vesicles were suspended in an external solution composed of the same NMDG-Cl solution. A pH gradient was initiated for each experiment through the addition of an NMDG base pulse (5 mM) which basified the external solution to pH 8.0, followed by the addition of the transporter as a DMSO solution (5  $\mu\text{L}$ ) at  $t = 0$  s. The ability of a transporter to dissipate the pH gradient through  $\text{H}^+/\text{Cl}^-$ -symport (or equivalent  $\text{OH}^-/\text{Cl}^-$  antiport) was determined through the change in the fluorescence emission spectra of HPTS. Efflux was measured for 210 s and treated with Triton X-100 to lyse the contents of the vesicle into the external solution and calibrate the 100%  $\text{Cl}^-$  efflux value. Detailed experimental methods, efflux plots and Hill fittings for each receptor can be found in the ESI. The  $\text{EC}_{50}$  values, Hill coefficients ( $n$ ) and ClogP are displayed in Table 2.

In general, the transport activity agreed with the expected trend whereby the receptors that possessed the strongest electron-withdrawing substituents (higher Hammett constants) facilitated the highest degree of  $\text{Cl}^-$  efflux. The lipophilicity of the receptors did not fully correlate with transport activity, presumably due to the simplistic level of calculation which could not consider the internal hydrogen bonding network.<sup>44</sup> The parent phenyl receptor **1** demonstrated the lowest activity and was found to be 65-times less active than compound **3**, which proved to be the most active transporter of the series with a calculated  $\text{EC}_{50}$  value of 0.05 mol% (Figure 6). Receptor **5** was shown to efficiently dissipate the pH gradient through  $\text{H}^+/\text{Cl}^-$  transport. Cyano groups are an effective appendage in the design of anion transporters due to their high  $\sigma_p$ . While the electron-withdrawing effects are similar to **3**, its lower transport ability may be governed by its lower

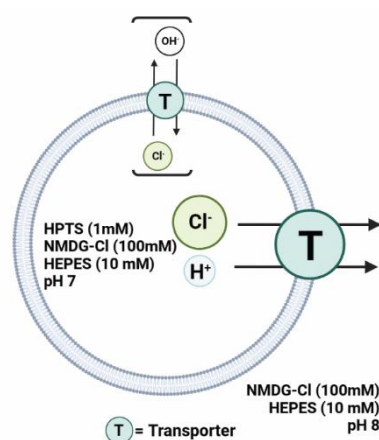


**Figure 4** Schematic of the HPTS fluorescence-based assay. POPC vesicles were loaded with HEPES (10 mM) buffered NMDG-Cl (100 mM) with HPTS (1 mM) and suspended in HEPES (10 mM) buffered NMDG-Cl (100 mM) and adjusted to pH 7. To start the experiment a base pulse of NMDG (0.5 M) was added to increase the external to pH 8.



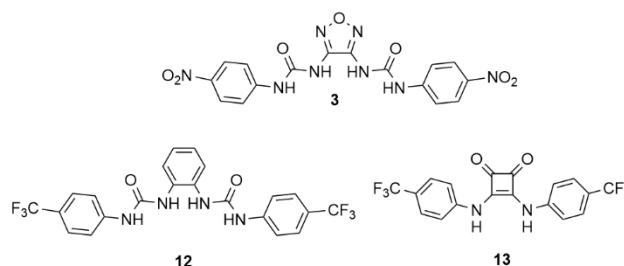
**Table 2** EC<sub>50</sub> values, Hill coefficients (*n*) and ClogP values for **1–9** in the NMDG-Cl assay

Compound	EC <sub>50</sub> <sup>a</sup>	<i>n</i>	ClogP <sup>b</sup>
<b>1</b>	3.23	0.8	2.8
<b>2</b>	0.24	0.5	4.8
<b>3</b>	0.05	0.9	3.4
<b>4</b>	0.51	1.1	3.6
<b>5</b>	0.07	1.3	2.5
<b>6</b>	0.55	1.2	6.9
<b>7</b>	0.38	0.9	8.1
<b>8</b>	1.05	1.1	4.6
<b>9</b>	0.13	0.7	6.8

<sup>a</sup> Effective concentration needed to obtain 50% Cl<sup>−</sup> efflux (EC<sub>50</sub>) at *t* = 200 s, reported in lipid to molar ratio (mol%). <sup>b</sup> Average ClogP values calculated using Flare (Cresset Group).

lipophilicity. Receptors with a high degree of fluorination also exhibited high activity. The presence of two bis-trifluoromethyl groups within compound **9** was found to increase the Cl<sup>−</sup> transport ability over receptors **2** and **7**. In addition to its higher binding affinity, compound **9** was hypothesised to sit in an optimal region of lipophilicity, whereby the calculated ClogP value of receptor **9** (ClogP = 6.8) was found to lie between that of **2** and **7** (ClogP = 4.8 and 8.1, respectively). Receptors **4** and **6** demonstrated comparable transport activity when compared to **8**, mirroring the results observed from the binding studies.

Due to the lack of anionophores constructed around a five-membered ring scaffold, the calculated EC<sub>50</sub> values of the furazan library were compared against scaffolds of differing geometries. It should be noted that the EC<sub>50</sub> values of the compared scaffolds have been scaled to account for the difference in lipid concentration between different assays to allow for a general comparison. The two most active furazan-based transporters, **3** and **5**, were found to be 10-times less active than the potent *ortho*-phenylene bis-urea **12** and

**Figure 6** *ortho*-Hydrogen bonding scaffolds. Furazan bis-urea **3** developed in this work, *ortho*-phenylene bis urea **12**, and squaramide **13**.

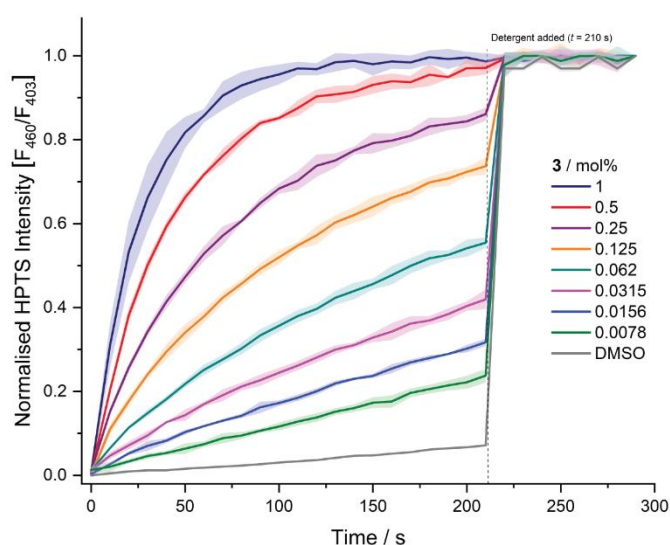
squaramide **13** (Figure 7), which has previously shown to induce apoptosis in cancerous cells.<sup>1,24,25</sup> Further comparison revealed the furazan bis-ureas to be comparable to that of the commonly used isophthalamide scaffold.<sup>45</sup>

The Hill coefficient quantifies the stoichiometry of the transport process where a value > 1 indicates a higher-order complex formation. If a transporter mediates Cl<sup>−</sup> transport as a mobile carrier, a value close to 1 is expected. This implies that one transporter binds to an anion in a 1:1 fashion and permits the translocation of the species across the lipid bilayer. Across all tested receptors, Hill coefficients were found to be ≈ 1, indicating the 1:1 mobile carrier process.

### Cell studies

Generally, furazan-containing compounds in medicinal chemistry inhibit enzymes that regulate cellular processes to disrupt function. This had led to their consideration as antibacterial, antiparasitic, antiviral and anticancer agents.<sup>46–50</sup> It should be noted that the furazan motif is typically not the pharmacophore, but its high electronegativity and multiple hydrogen bond acceptors are used to further enhance activity or selectivity relative to other heterocycles or bioisosteres.<sup>30</sup> Synthetic anion transporters have been proposed as a novel strategy for the treatment of cancer, therefore, taken together with the previously explored bioactivity of furazan containing compounds, cell viability studies of anionophores **1–9** were conducted.

The cytotoxicity of the library was assessed using the 3-(4,5-dimethylthiazol-2-yl)-2,5-diphenyltetrazolium bromide (MTT) cell viability assay against a normal cell line, human embryo kidney cells (HEK293), and a triple-negative mouse breast (4T1) cancer cell line (Table 3). After 24 h of incubation, only receptor **5** was shown to be non-toxic towards both cell lines. The remaining anionophores showed potency to both cell lines with varying degrees of cytotoxicity. No notable discrimination in cytotoxicity was observed between the normal and cancerous cell lines as was expected due to the simple nature of the receptors. In cancerous cells, the most active transporters were generally shown to exhibit the highest toxicities. In addition, a comparison of the Hammett constants against the IC<sub>50</sub> values revealed a strong trend in cytotoxicity, evidence that the high electron-withdrawing strength of the peripheral phenyl rings,

**Figure 7** Dose response studies for receptor **3** using the HPTS fluorescence-based assay. Each data point is the average of three repeats with error bars to show standard deviation.

**Table 3** Half maximum inhibitory concentration ( $IC_{50}$ ,  $\mu M$ ) values upon incubation of **1–9** in human embryo kidney cells (HEK293) and triple-negative mouse breast cancer cells (4T1) for 24 h.

Compound	$IC_{50}$ (HEK293) <sup>a</sup>	$IC_{50}$ (4T1) <sup>a</sup>
<b>1</b>	37.6	99.4
<b>2</b>	46.5	25.0
<b>3</b>	41.0	13.9
<b>4</b>	32.5	64.4
<b>5</b>	>200	>200
<b>6</b>	28.3	56.0
<b>7</b>	16.8	19.2
<b>8</b>	47.4	14.0
<b>9</b>	12.7	10.3

<sup>a</sup> half maximum inhibitory concentration ( $IC_{50}$ ,  $\mu M$ ) values

and their effect on NH acidity, are important components in eliciting a physiological response. Receptor **9** showed the highest potency, followed by compounds **3**, **8**, and **7**. It was found that the receptors with a lower degree of fluorination exhibited a less significant effect on the toxicity in the cancerous cell line.

The trends were less prevalent in the normal cell line. Receptor **9** was shown again to possess the highest cytotoxicity, with similar activity to the cancerous cell line. Fluorinated compounds **7**, **6**, and **4** were also found to exhibit moderately high antiproliferative activity, indicating that the lipophilicity of the receptor may also play a role in the toxicity of the bis-urea. With the exception of compound **5**, the remaining receptors demonstrated reasonable and comparable cytotoxicities towards the normal cell line.

## Conclusions

A series of nine bis-ureas were prepared using a novel central scaffold through synthetically accessible one- or two-step procedures. It was proposed that the receptors exist in a *syn–syn* conformation in the solution state. However, upon anion coordination a conformation switch occurs to form the *anti–anti* orientation, driven by a network of internal hydrogen bonds which added complexity to the assessment of lipophilicity. The preorganised nature of the ureas through intramolecular hydrogen bonding was attributed to the modest  $Cl^-$  binding affinity. Mechanistic studies revealed the transporters to function predominantly as  $H^+/Cl^-$  cotransporters which perturbed pH gradients in a liposomal fluorescence-based assay. Almost all transporters demonstrated cytotoxicity towards HEK293 and 4T1 cell lines after 24 h. Additionally, anionophores with the strongest electron-withdrawing substituents generally exhibited the highest cytotoxicity in the cancerous 4T1 cell line. Despite the challenges posed by the distinctive preorganized geometry of the furazan scaffold, its anionophoric capability shows potential for the further exploration of synthetically accessible novel architectures that can effectively facilitate anion transport.

## Author Contributions

W.G.R. and E.G.W. conducted the synthesis. W.G.R., E.G.W., K.T. and D.A.M. performed the anion binding, transport, and spectroscopic data curation; L.C. performed the cellular studies; M.F. conducted the crystallography; W.G.R. wrote the original draft; P.A.G. conceptualised the project, provided supervision, manuscript review and editing.

## Conflicts of interest

There are no conflicts to declare.

## Acknowledgements

W.G.R., E.G.W., M.F., D.A.M., K.T., and P.A.G. acknowledge and pay respect to the Gadigal people of the Eora Nation, the traditional owners of the land on which we research, teach, and collaborate at The University of Technology Sydney and the University of Sydney. P.A.G. thanks The Australian Research Council (DP200100453) and The University of Technology Sydney for funding. L.C., and C.Y. acknowledge the facilities and the scientific and technical assistance of the Australian Microscopy & Microanalysis Research Facility at the Centre for Microscopy and Microanalysis at The University of Queensland. W.G.R. gratefully acknowledges financial support through the Paulette Isabel Jones Career Award at the University of Sydney. Figures 3 and 5 were created with BioRender.com.

## Notes and references

1. S. H. Park, S. H. Park, E. N. W. Howe, J. Y. Hyun, L. J. Chen, I. Hwang, G. Vargas-Zuniga, N. Busschaert, P. A. Gale, J. L. Sessler and I. Shin, Determinants of Ion-Transporter Cancer Cell Death, *Chem*, 2019, **5**, 2079–2098.
2. V. Soto-Cerrato, P. Manuel-Manresa, E. Hernando, S. Calabuig-Farinas, A. Martinez-Romero, V. Fernandez-Duenas, K. Sahlholm, T. Knopf, M. Garcia-Valverde, A. M. Rodilla, E. Jantus-Lewintre, R. Farras, F. Ciruela, R. Perez-Tomas and R. Quesada, Facilitated Anion Transport Induces Hyperpolarization of the Cell Membrane That Triggers Differentiation and Cell Death in Cancer Stem Cells, *J. Am. Chem. Soc.*, 2015, **137**, 15892–15898.
3. L. A. Jowett, E. N. W. Howe, V. Soto-Cerrato, W. Van Rossom, R. Perez-Tomas and P. A. Gale, Indole-based perenosins as highly potent HCl transporters and potential anti-cancer agents, *Sci. Rep.*, 2017, **7**, 9397.
4. S. Kubik, R. Kirchner, D. Nolting and J. Seidel, A molecular oyster: a neutral anion receptor containing two cyclopeptide subunits with a remarkable sulfate affinity in aqueous solution, *J. Am. Chem. Soc.*, 2002, **124**, 12752–12760.
5. J. Svec, M. Necas and V. Sindelar, Bambus[6]uril, *Angew. Chem. Int. Ed.*, 2010, **49**, 2378–2381.
6. C. Raposo, M. Almaraz, M. Martín, V. Weinrich, M. L. Mussóns, V. Alcázar, M. C. Caballero and J. R. Morán, Tris(2-aminoethyl)amine, a Suitable Spacer for Phosphate and Sulfate Receptors, *Chem. Lett.*, 1995, **24**, 759–760.
7. J. I. Bruce, R. S. Dickins, L. J. Govenlock, T. Gunnlaugsson, S. Lopinski, M. P. Lowe, D. Parker, R. D. Peacock, J. J. B. Perry, S. Aime and M. Botta, The Selectivity of Reversible Oxy-

- Anion Binding in Aqueous Solution at a Chiral Europium and Terbium Center: Signaling of Carbonate Chelation by Changes in the Form and Circular Polarization of Luminescence Emission, *J. Am. Chem. Soc.*, 2000, **122**, 9674-9684.
8. P. G. Young, J. K. Clegg, M. Bhadbhade and K. A. Jolliffe, Hybrid cyclic peptide-thiourea cryptands for anion recognition, *Chem. Commun.*, 2011, **47**, 463-465.
  9. P. A. Gale, J. L. Sessler, V. Král and V. Lynch, Calix[4]pyrroles: Old Yet New Anion-Binding Agents, *J. Am. Chem. Soc.*, 1996, **118**, 5140-5141.
  10. J. F. Ayme, J. E. Beves, C. J. Campbell, G. Gil-Ramirez, D. A. Leigh and A. J. Stephens, Strong and Selective Anion Binding within the Central Cavity of Molecular Knots and Links, *J. Am. Chem. Soc.*, 2015, **137**, 9812-9815.
  11. M. J. Langton, S. W. Robinson, I. Marques, V. Felix and P. D. Beer, Halogen bonding in water results in enhanced anion recognition in acyclic and rotaxane hosts, *Nat. Chem.*, 2014, **6**, 1039-1043.
  12. A. Ojida, I. Takashima, T. Kohira, H. Nonaka and I. Hamachi, Turn-on fluorescence sensing of nucleoside polyphosphates using a xanthene-based Zn(II) complex chemosensor, *J. Am. Chem. Soc.*, 2008, **130**, 12095-12101.
  13. L. M. Lee, M. Tsemperouli, A. I. Poblador-Bahamonde, S. Benz, N. Sakai, K. Sugihara and S. Matile, Anion Transport with Pnictogen Bonds in Direct Comparison with Chalcogen and Halogen Bonds, *J. Am. Chem. Soc.*, 2019, **141**, 810-814.
  14. J. T. Davis, P. A. Gale, O. A. Okunola, P. Prados, J. C. Iglesias-Sanchez, T. Torroba and R. Quesada, Using small molecules to facilitate exchange of bicarbonate and chloride anions across liposomal membranes, *Nat. Chem.*, 2009, **1**, 138-144.
  15. D. Mondal, M. Ahmad, B. Dey, A. Mondal and P. Talukdar, Formation of supramolecular channels by reversible unwinding-rewinding of bis(indole) double helix via ion coordination, *Nat Commun.*, 2022, **13**, 6507.
  16. L. E. Bickerton, A. J. Sterling, P. D. Beer, F. Duarte and M. J. Langton, Transmembrane anion transport mediated by halogen bonding and hydrogen bonding triazole anionophores, *Chem. Sci.*, 2020, **11**, 4722-4729.
  17. C. M. Dias, H. Valkenier and A. P. Davis, Anthracene Bisureas as Powerful and Accessible Anion Carriers, *Chem. Eur. J.*, 2018, **24**, 6262-6268.
  18. D. A. McNaughton, W. G. Ryder, A. M. Gilchrist, P. Wang, M. Fares, X. Wu and P. A. Gale, New insights and discoveries in anion receptor chemistry, *Chem*, 2023, **9**, 3045-3112.
  19. S. Hussain, P. R. Brotherhood, L. W. Judd and A. P. Davis, Diaxial diureido decalins as compact, efficient, and tunable anion transporters, *J. Am. Chem. Soc.*, 2011, **133**, 1614-1617.
  20. Y. Li and A. H. Flood, Pure C-H hydrogen bonding to chloride ions: a preorganized and rigid macrocyclic receptor, *Angew. Chem. Int. Ed.*, 2008, **47**, 2649-2652.
  21. A. V. Koulov, T. N. Lambert, R. Shukla, M. Jain, J. M. Boon, B. D. Smith, H. Li, D. N. Sheppard, J. B. Joos, J. P. Clare and A. P. Davis, Chloride transport across vesicle and cell membranes by steroid-based receptors, *Angew. Chem. Int. Ed.*, 2003, **42**, 4931-4933.
  22. P. A. Gale, J. T. Davis and R. Quesada, Anion transport and supramolecular medicinal chemistry, *Chem. Soc. Rev.*, 2017, **46**, 2497-2519.
  23. M. Fares, X. Wu, D. A. McNaughton, A. M. Gilchrist, W. Lewis, P. A. Keller, A. Arias-Betancur, P. Fontova, R. Perez-Tomas and P. A. Gale, A potent fluorescent transmembrane HCl transporter perturbs cellular pH and promotes cancer cell death, *Org. Biomol. Chem.*, 2023, **21**, 2509-2515.
  24. L. E. Karagiannidis, C. J. Haynes, K. J. Holder, I. L. Kirby, S. J. Moore, N. J. Wells and P. A. Gale, Highly effective yet simple transmembrane anion transporters based upon ortho-phenylenediamine bis-ureas, *Chem. Commun.*, 2014, **50**, 12050-12053.
  25. N. Busschaert, I. L. Kirby, S. Young, S. J. Coles, P. N. Horton, M. E. Light and P. A. Gale, Squaramides as Potent Transmembrane Anion Transporters, *Angew. Chem. Int. Ed.*, 2012, **124**, 4502-4506.
  26. A. Jeppesen, B. E. Nielsen, D. Larsen, O. M. Akselsen, T. I. Solling, T. Brock-Nannestad and M. Pittelkow, Croconamides: a new dual hydrogen bond donating motif for anion recognition and organocatalysis, *Org. Biomol. Chem.*, 2017, **15**, 2784-2790.
  27. V. E. Zwicker, K. K. Y. Yuen, D. G. Smith, J. Ho, L. Qin, P. Turner and K. A. Jolliffe, Deltamides and Croconamides: Expanding the Range of Dual H-bond Donors for Selective Anion Recognition, *Chem. Eur. J.*, 2018, **24**, 1140-1150.
  28. A. E. Lutskii, A. V. Shepel, O. P. Shvaika and G. P. Klimisha, Dipole moments and the structure of the molecules of some oxadiazole derivatives, *Chem. Heterocycl. Compd.*, 1972, **5**, 343-348.
  29. J. Bostrom, A. Hogner, A. Llinas, E. Wellner and A. T. Plowright, Oxadiazoles in medicinal chemistry, *J. Med. Chem.*, 2012, **55**, 1817-1830.
  30. R. S. Mancini, C. J. Barden, D. F. Weaver and M. A. Reed, Furazans in Medicinal Chemistry, *J. Med. Chem.*, 2021, **64**, 1786-1815.
  31. A. B. Sheremetev, The chemistry of furazans fused to six- and seven-membered heterocycles with one heteroatom, *Russ. Chem. Rev.*, 1999, **68**, 137-148.
  32. N. Busschaert, M. Wenzel, M. E. Light, P. Iglesias-Hernandez, R. Perez-Tomas and P. A. Gale, Structure-activity relationships in tripodal transmembrane anion transporters: the effect of fluorination, *J. Am. Chem. Soc.*, 2011, **133**, 14136-14148.
  33. D. A. McNaughton, L. K. Macreadie and P. A. Gale, Acridinone-based anion transporters, *Org. Biomol. Chem.*, 2021, **19**, 9659-9674.
  34. C. J. Haynes, N. Busschaert, I. L. Kirby, J. Herniman, M. E. Light, N. J. Wells, I. Marques, V. Felix and P. A. Gale, Acylthioureas as anion transporters: the effect of intramolecular hydrogen bonding, *Org. Biomol. Chem.*, 2014, **12**, 62-72.
  35. <https://app.supramolecular.org>.
  36. D. Hibbert and P. Thordarson, The death of the Job plot, transparency, open science and online tools, uncertainty estimation methods and other developments in supramolecular chemistry data analysis, *Chem. Commun.*, 2016, **52**, 12792-12805.
  37. C. Hansch, A. Leo and R. W. Taft, A survey of Hammett substituent constants and resonance and field parameters, *Chem. Rev.*, 2002, **91**, 165-195.
  38. R. J. De Pasquale and C. Tamborski, Reactions of sodium pentafluorophenolate with substituted pentafluorobenzenes, *J. Org. Chem.*, 2002, **32**, 3163-3168.



39. J. M. Lehn, Supramolecular Chemistry—Scope and Perspectives Molecules, Supermolecules, and Molecular Devices (Nobel Lecture), *Angewandte Chemie International Edition in English*, 1988, **27**, 89-112.
40. M. J. Spooner and P. A. Gale, Anion transport across varying lipid membranes—the effect of lipophilicity, *Chem. Commun.*, 2015, **51**, 4883-4886.
41. N. J. Knight, E. Hernando, C. J. E. Haynes, N. Busschaert, H. J. Clarke, K. Takimoto, M. Garcia-Valverde, J. G. Frey, R. Quesada and P. A. Gale, QSAR analysis of substituent effects on tambjamine anion transporters, *Chem. Sci.*, 2016, **7**, 1600-1608.
42. V. Saggiomo, S. Otto, I. Marques, V. Felix, T. Torroba and R. Quesada, The role of lipophilicity in transmembrane anion transport, *Chem Commun (Camb)*, 2012, **48**, 5274-5276.
43. A. M. Gilchrist, P. Wang, I. Carreira-Barral, D. Alonso-Carrillo, X. Wu, R. Quesada and P. A. Gale, Supramolecular methods: the 8-hydroxypyrene-1,3,6-trisulfonic acid (HPTS) transport assay, *Supramol. Chem.*, 2021, **33**, 325-344.
44. It should be noted that the lipophilicity of the furazan bis-ureas are determined by both the substitution effects on the phenyl rings and the formation and strength of the intramolecular hydrogen bonds that drive its preorganised geometry. Therefore, the ClogP values have been treated with caution as they do not consider the presence of intramolecular hydrogen bonds and their associated level of solvent inaccessibility.
45. G. Picci, I. Carreira-Barral, D. Alonso-Carrillo, D. Sanz-González, P. Fernández-López, M. García-Valverde, C. Caltagirone and R. Quesada, Simple isophthalamides/dipicolineamides as active transmembrane anion transporters, *Supramol. Chem.*, 2019, **32**, 112-118.
46. M. Pagano, D. Castagnolo, M. Bernardini, A. L. Fallacara, I. Laurenzana, D. Deodato, U. Kessler, B. Pilger, L. Stergiou, S. Strunze, C. Tintori and M. Botta, The fight against the influenza A virus H1N1: synthesis, molecular modeling, and biological evaluation of benzofurazan derivatives as viral RNA polymerase inhibitors, *ChemMedChem*, 2014, **9**, 129-150.
47. A. Cameron, J. Read, R. Tranter, V. J. Winter, R. B. Sessions, R. L. Brady, L. Vivas, A. Easton, H. Kendrick, S. L. Croft, D. Barros, J. L. Lavandera, J. J. Martin, F. Risco, S. Garcia-Ochoa, F. J. Gamon, L. Sanz, L. Leon, J. R. Ruiz, R. Gabarro, A. Mallo and F. Gomez de las Heras, Identification and activity of a series ofazole-based compounds with lactate dehydrogenase-directed anti-malarial activity, *J. Biol. Chem.*, 2004, **279**, 31429-31439.
48. I. V. Galkina, G. L. Takhautdinova, E. V. Tudrii, L. M. Yusupova, I. F. Falyakhov, O. K. Pozdeev, M. P. Shulaeva, L. V. Kipenskaya, V. G. Sakhibullina, D. B. Krivolapov, I. A. Litvinov, V. I. Galkin and R. A. Cherkasov, Synthesis, structure, and antibacterial activity of aminobenzofuroxan and aminobenzofurazan, *Russ. J. Org. Chem.*, 2013, **49**, 591-597.
49. F. S. Levinson, M. I. Evgen'ev, E. A. Ermolaeva, S. I. Efimov, T. V. Garipov and R. G. Karimova, Synthesis and Biological Activity of Arylamino-substituted Nitrobenzodifurazans, *Pharm. Chem. J.*, 2003, **37**, 578-581.
50. A. Sharma, A. Broggini-Tenzer, V. Vuong, A. Messikommer, K. J. Nytko, M. Guckenberger, F. Bachmann, H. A. Lane and M. Pruschy, The novel microtubule targeting agent BAL101553 in combination with radiotherapy in treatment-refractory tumor models, *Radiother. Oncol.*, 2017, **124**, 433-438.

TOC graphic text: A five-membered heterocyclic ring was used as a central scaffold to develop a series of anion receptors. The library perturbed liposomal pH gradients through H<sup>+</sup>/Cl<sup>-</sup> transmembrane transport and elicited a variety of cytotoxicities against normal and cancerous cell lines.